

Partition-function-zero analysis of polymer adsorption for a continuum chain modelMark P. Taylor^{*} and Samip Basnet*Department of Physics, Hiram College, Hiram, Ohio 44234, USA*Jutta Luettmmer-Strathmann[†]*Departments of Physics and Chemistry, University of Akron, Akron, Ohio 44325, USA*

(Received 2 August 2021; accepted 13 September 2021; published 27 September 2021)

Polymer chains undergoing adsorption are expected to show universal critical behavior which may be investigated using partition function zeros. The focus of this work is the adsorption transition for a continuum chain, allowing for investigation of a continuous range of the attractive interaction and comparison with recent high-precision lattice model studies. The partition function (Fisher) zeros for a tangent-hard-sphere N -mer chain (monomer diameter σ) tethered to a flat wall with an attractive square-well potential (range $\lambda\sigma$, depth ϵ) have been computed for chains up to $N = 1280$ with $0.01 \leq \lambda \leq 2.0$. In the complex-Boltzmann-factor plane these zeros are concentrated in an annular region, centered on the origin and open about the real axis. With increasing N , the leading zeros, $w_1(N)$, approach the positive real axis as described by the asymptotic scaling law $w_1(N) - y_c \sim N^{-\phi}$, where $y_c = e^{\epsilon/k_B T_c}$ is the critical point and T_c is the critical temperature. In this work, we study the polymer adsorption transition by analyzing the trajectory of the leading zeros as they approach y_c in the complex plane. We use finite-size scaling (including corrections to scaling) to determine the critical point and the scaling exponent ϕ as well as the approach angle θ_c , between the real axis and the leading-zero trajectory. Variation of the interaction range λ moves the critical point, such that T_c decreases with λ , while the results for ϕ and θ_c are approximately independent of λ . Our values of $\phi = 0.479(9)$ and $\theta_c = 56.8(1.4)^\circ$ are in agreement with the best lattice model results for polymer adsorption, further demonstrating the universality of these constants across both lattice and continuum models.

DOI: [10.1103/PhysRevE.104.034502](https://doi.org/10.1103/PhysRevE.104.034502)**I. INTRODUCTION**

The reversible adsorption of a flexible polymer chain to an attractive surface is an important problem in polymer, materials, and surface science [1]. For a long chain this adsorption transition is a second-order phase transition, characterized by universal critical exponents. Of particular interest for the polymer adsorption problem is the so called crossover exponent ϕ which governs the number of adsorbed sites for a N -mer chain at the transition via the asymptotic scaling behavior $n_a(T_c) \sim N^\phi$, where T_c is the transition temperature in the thermodynamic ($N \rightarrow \infty$) limit. In one of the first comprehensive studies of this transition Eisenriegler *et al.* estimated this exponent to have the value $\phi = 0.58(2)$ [2]. Over the past several decades the details of the polymer adsorption transition have remained a topic of active theoretical interest [3–20]. In particular, until recently, there has been a persistent lack of consensus as to the exact value of the exponent ϕ with values being reported in the range $0.4 \leq \phi \leq 0.67$. It was clear that system size was a limiting issue in accurate determination of the critical temperature T_c and that the ϕ estimates are quite sensitive to the T_c estimate [7,9]. It was also suggested that ϕ might be super-universal, with its value

in three dimensions matching the exactly known value in two and four dimensions of $\phi = 1/2$ [4–6].

With advances in both simulation algorithms and computer hardware, longer chain lengths have become accessible and Grassberger, studying an absorbing chain on the simple cubic lattice using the PERM algorithm for chains up to length $N = 8000$, obtained the result $\phi = 0.484(2)$ [8]. Grassberger's value of $\phi < 0.5$, which implies a nondiverging specific heat at the transition, has now been confirmed in a number of studies (all using the simple cubic lattice model) [13,18–20], although there remains a small spread in the reported results not covered by the estimated statistical errors. The recent work by Bradly *et al.* [19] has shown that for both two- and three-dimensional lattice chains different approaches to obtaining T_c can lead to ϕ estimates whose scatter is larger than the estimated statistical uncertainty for each approach.

Recent lattice model studies have investigated the effects of a wide range of conditions on the adsorption transition, including chain stiffness [12], range of the attractive interaction [13], and solvent conditions [18–21]. Due to the larger computational effort required for off-lattice models, simulations of continuum chains have been restricted to shorter chain lengths, which makes the determination of the crossover exponent more difficult. Studying a bead-spring model with Monte Carlo simulations, Metzger *et al.* [5] found a value of $\phi = 0.50 \pm 0.02$, which is consistent with the best lattice model results. Bhattacharya *et al.* [22,23] derived limits on the

^{*}taylormp@hiram.edu[†]jutta@uakron.edu

crossover exponent, $0.34 \leq \phi \leq 0.59$, from a theory for the desorption transition under pulling and confirmed their findings with Monte Carlo simulations. More recently, Milchev and Binder [24,25] investigated the effect of chain stiffness on the adsorption transition with molecular dynamics simulations of a bead-spring model and find results consistent with $\phi = 0.48$ for chains that are not too stiff, in agreement with lattice model results for semiflexible chains [12]. Off-lattice insight into the adsorption of stiffer polymers (filaments) has also been gained through theory and simulations of wormlike chains [26–28]. These studies confirm that the adsorption transition of semiflexible chains is continuous [26,27] and that the transition temperature increases with chain stiffness and the range of the attractive surface interaction [26–28].

In the present work, we study the adsorption transition with a continuum model for a flexible chain in good solvent tethered to an attractive surface. The polymer is represented by a hard-sphere chain with bond length equal to the chain diameter σ and the attractive interaction is described by a square well of fixed depth ϵ and variable range $\lambda\sigma$. This is a coarse-grained model, where each bead of the chain represents several monomers of a typical polymer, which implies that interaction ranges of common surface systems are smaller than a bead diameter. To cover this physically relevant range, we simulate square wells with $0.01 \leq \lambda \leq 2.0$.

Since the development of the Yang-Lee theory of phase transitions in the grand-canonical ensemble [29,30], its extension to the canonical ensemble by Fisher [31], and detailed examination of finite systems by Itzykson *et al.* [32], partition function zeros have been analyzed to study phase transitions in a wide range of systems [33] including a number of studies on the collapse and adsorption transitions for chain molecules [15,17,34–41]. In our previous work, we used the zeros of the canonical partition function (Fisher zeros) to investigate the polymer adsorption transition in good solvent for a bond-fluctuation (BF) lattice model [15]. The Fisher zeros for this lattice model are concentrated in an annular region centered on the origin of the complex plane. With increasing chain length, the leading zeros approach the critical point on the positive real axis, following an asymptotic scaling law that involves the crossover exponent ϕ . Our finite-size-scaling analysis for this model, which did not systematically include corrections to scaling, led to inconclusive results regarding the value of ϕ relative to $1/2$ with our best estimate being $\phi = 0.515(25)$. In the present work we present a more robust finite-size-scaling analysis of the partition function zeros that *does* systematically include corrections to scaling (whose importance has been pointed out by both Plascak *et al.* [18] and Bradly *et al.* [19]). We apply this approach to the continuum hard-sphere-chain model (and also use it to reanalyze the BF-lattice model) and find results that are both internally consistent and in agreement with the most recent lattice model studies.

In summary, the goals of the present work are threefold. First, presentation of a new method (partition-function-zero analysis including systematic corrections to scaling) to study the polymer adsorption transition. Second, analysis of a continuum model in order to compare with the existing high precision lattice model studies of polymer adsorption. And third, analysis of chain adsorption as a function of a

continuously variable interaction range λ (including $\lambda < \sigma$, which is not possible with a lattice model).

II. THEORY AND METHODS

A. HS chain model

The model studied here is a flexible continuum chain composed of N tangent hard spheres of diameter σ , tethered at one end to a flat wall with an attractive square-well (SW) potential of range $\lambda\sigma$. The chain is confined to the positive half-space $z > 0$ and the interaction between chain-monomer i and the wall is given by

$$u_i(z) = \begin{cases} -\epsilon & 0 \leq z \leq \lambda\sigma \\ 0 & z > \lambda\sigma \end{cases}, \quad (1)$$

where z is the minimum vertical distance between the bead surface and the wall. The chain energy is given by $E_n = -n\epsilon$, where n is the number of adsorbed sites (i.e., the number of sites with $z < \lambda\sigma$, including the tethered site for which $z = 0$) such that $[\lambda + 1] \leq n \leq N$ where $[]$ denotes integer part.

B. Simulation methods

We construct the density of states $g(E_n)$ for the tethered HS-chain model using the Wang-Landau algorithm [42,43]. In this iterative approach, one samples configuration space using a set of Monte Carlo moves with an acceptance probability based on the current estimate of the density of states given by

$$P_{\text{accept}}(a \rightarrow b) = \min\left(1, \frac{g(E_a)}{g(E_b)}\right). \quad (2)$$

After each move attempt the density of states estimate for the current state (call it E_c) is modified by a factor $f_k > 1$ [$\ln g(E_c) \rightarrow f_k \ln g(E_c)$] and the entry in a state visitation histogram $H(E)$ for that state is incremented [$H(E_c) \rightarrow H(E_c) + 1$]. The $H(E)$ histogram is periodically checked for “flatness” which indicates a uniform sampling of all accessible energy states. When flatness is achieved, simulation level k ends, the modification factor is reduced ($f_{k+1} = \sqrt{f_k}$), the visitation histogram is zeroed [$H(E) = 0 \forall E$], and simulation level $k + 1$ begins. Our move set consists of single-bead axial rotations, standard pivots and pivots about the z axis, segment reflection, cut and permute, and end-bridging (which requires additional weight factors in P_{accept}) [44–47]. We start the simulations with $f_0 = e^1$ assuming a uniform density of states [$g(E_n) = 1 \forall n$], use a flatness criterion in the range 1% \rightarrow 20% depending on chain length, and run the simulations for $k = 30$ levels of iteration. To assess simulation uncertainty, we typically run 10 or more independent versions of each simulation.

C. Partition function zeros

The canonical partition function for a system with a discrete energy spectrum, with energy states $E_n = -n\epsilon$ ($1 \leq n \leq N$) is given by

$$Z_N(T) = \sum_{n=1}^N g(E_n) e^{-E_n/k_B T} = g_1 y \sum_{n=0}^{N-1} (g_{n+1}/g_1) y^n, \quad (3)$$

where $g_n = g(E_n)$ is the density of states for energy level E_n and $y = e^{\epsilon/k_B T}$ (where k_B is the Boltzmann constant and T is the temperature). The above expression is a polynomial in y which can be rewritten in product form in terms of its $N - 1$ roots or zeros as

$$Z_N(T) = g_1 y \prod_{k=1}^{N-1} (y - w_k). \quad (4)$$

where the complex zeros (known as Fisher zeros) come in conjugate pairs $w_k = a \pm ib$ such that any real roots $w_k = a_k$ lie on the negative axis (since the g_n are all positive).

In the Yang-Lee theory of phase transitions [29,30] some partition function zeros approach the positive real axis with increasing system size, moving onto the real axis at a point y_c in the thermodynamic limit ($N \rightarrow \infty$). This results in nonanalytic behavior in the thermodynamic functions at the transition point $y = y_c$. While the Yang-Lee theory was developed within the grand-canonical ensemble, the same description holds for the canonical ensemble Fisher zeros [31]. Thus, the Helmholtz free energy, given by

$$F_N(T)/k_B T = -\ln Z_N(T) = -\ln(g_1 y) - \sum_{k=1}^{N-1} \ln(y - w_k), \quad (5)$$

will become nonanalytic for $N \rightarrow \infty$ as some zeros move onto the real axis (i.e., some $w_k \rightarrow y_c$). Here we focus on the leading zero which we denote w_1 and define as the Fisher zero in the first quadrant with the smallest imaginary part. For polymer adsorption, the order parameter for the transition is given by the fraction of adsorbed monomers $M_N = n_a/N$ where $n_a = \langle n \rangle = |\langle E_n \rangle|/\epsilon$. This order parameter can be written as a temperature derivative of $F_N(T)$ as follows:

$$M_N(T) = \frac{y}{N} \left| \frac{\partial(F_N/k_B T)}{\partial y} \right| = \frac{1}{N} \left[1 + \sum_{k=1}^{N-1} \frac{y}{(y - w_k)} \right] \quad (6)$$

and thus also becomes nonanalytic for $w_1 \rightarrow y_c = e^{\epsilon/k_B T_c}$ (as $N \rightarrow \infty$). For large N , $M_N(T)$ will be governed at $T = T_c$ by the leading zero, resulting in the asymptotic behavior

$$M_N(T_c) \sim \frac{1}{N} |y_c - w_1|^{-1}. \quad (7)$$

D. Finite-size scaling

The scaling of the polymer adsorption order parameter with system size defines the crossover exponent ϕ via $M_N(T_c) \sim N^{\phi-1}$ [2] and thus, Eq. (7) implies an asymptotic scaling behavior for the leading partition function zero of [32]

$$y_c - w_1 \sim N^{-\phi}. \quad (8)$$

Here we will assume a finite-size scaling expression [48–50] for the leading zero, valid in the complex plane, given by

$$w_1(N) = y_c + DN^{-\phi}(1 + dN^{-\Delta}), \quad (9)$$

where $D = D_r + iD_i$ and $d = d_r + id_i$ are complex constants and the exponent Δ describes the lowest-order correction-to-scaling contribution. Exploiting the fact that Eq. (9) is complex, we can eliminate the $N^{-\phi}$ dependence by an appropriate combination of real and imaginary parts which,

retaining terms to first order in $N^{-\Delta}$, yields the relation

$$\text{Re}[w_1(N)] = y_c + m \text{Im}[w_1(N)](1 + cN^{-\Delta}), \quad (10)$$

where $m = D_r/D_i$ and $c = -d_i(m^2 + 1)/m$ are real constants. In the absence of any correction to scaling (i.e., $d = 0$, $c = 0$), a plot of $\text{Im}[w_1]$ vs $\text{Re}[w_1]$ will yield a straight line with the leading zeros approaching the critical point y_c at an angle of $\theta_c = \tan^{-1}(1/m)$. (This approach angle, which derives from an amplitude ratio, is expected to exhibit universal behavior [32,49,51]). Alternatively, any curvature in such a plot indicates corrections to scaling are needed. We also note that, to first order in $N^{-\Delta}$, Eq. (10) can be rewritten as

$$\text{Re}[w_1] = y_c + \alpha_1 \text{Im}[w_1] + \alpha_2 (\text{Im}[w_1])^2 N^{\phi-\Delta} \quad (11)$$

and thus if $\phi = \Delta$, $\text{Re}[w_1]$ will be quadratic in $\text{Im}[w_1]$. Such behavior has been noted for lattice polymers [15,17] and is consistent with the value $\phi \approx 0.5$ and the general assumption that $\Delta = 0.5$ [8,13,18].

In the calculations presented below we use Eq. (10), assuming $\Delta = 0.5$, to determine the critical point y_c and approach angle θ_c . We then return to Eq. (9) and determine the crossover exponent through the scaling of the absolute distance of the leading zeros from the critical point which can be written, to first order in $N^{-\Delta}$, as

$$|w_1 - y_c| = AN^{-\phi}(1 + BN^{-\Delta}). \quad (12)$$

where $A = \sqrt{D_r^2 + D_i^2}$ and $B = d_r$ are real constants and the distance is given by $|w_1 - y_c| = \{(\text{Re}[w_1] - y_c)^2 + (\text{Im}[w_1])^2\}^{1/2}$. The four fit parameters m , c , A , and B allow determination of the parameter set D_r , D_i , d_r , and d_i . The above analysis for the complex w plane can be mapped onto the complex inverse temperature plane given by

$$\ln(w) = \ln(a + ib) = \beta + i\tau, \quad (13)$$

where $\beta = \epsilon/k_B T = \ln(a^2 + b^2)^{1/2}$ and $\tau = \tan^{-1}(b/a)$. The scaling relations given in Eqs. (8)–(12) hold in the $\beta\tau$ -complex plane with the substitutions of $w_1 \rightarrow \beta_1 + i\tau_1$, $y_c \rightarrow \beta_c$, and $A \rightarrow A/y_c$. Since this is a conformal mapping the approach angle θ_c is expected to be preserved.

It is also possible to determine the crossover exponent ϕ without first locating the critical point, by either simply carrying out a curve fit to the imaginary part of Eq. (9) (or its $\beta\tau$ plane analog) or to use the imaginary part of the leading zeros to construct a sequence of finite-size approximates to ϕ via the ratio [13]

$$\phi_{\text{eff}}(N) = \frac{1}{\ln 4} \ln \left\{ \frac{\text{Im}[z(N/2)]}{\text{Im}[z(2N)]} \right\} \quad (14)$$

for either the $z = w_1$ or $z = \beta_1 + i\tau_1$ zeros. With the lowest-order correction to scaling, retaining terms to first order in $N^{-\Delta}$, these $\phi_{\text{eff}}(N)$ estimates approach the asymptotic value ϕ according to

$$\phi_{\text{eff}}(N) = \phi + \frac{A_1}{N^\Delta}, \quad (15)$$

where $A_1 = (d_r + md_i)(2^{2\Delta} - 1)/(2^\Delta \ln 4)$.

III. RESULTS

Here we present results for the adsorption transition of HS chains up to length $N = 1280$ tethered to an attractive surface with SW interaction ranges $\lambda = 0.01, 0.1, 0.5, 1.0$, and 2.0 . For comparison, we also present a reanalysis of results for the bond-fluctuation lattice model studied previously [15]. The partition function zeros are computed from the density of states using Mathematica. For $N > 512$ we run the WL simulations across a reduced energy range (with $n_{\max} \geq N/2$ surface contacts). For long chains the adsorption transition occurs at $\langle n \rangle \ll N/2$, and we find that this truncated energy range gives accurate estimates of the leading partition function zero [15].

In Fig. 1 we show the partition function zeros for the case of $N = 512$, $\lambda = 0.5$ in the complex w plane (noting that some zeros fall outside the bounds of this figure). The zeros are seen to be concentrated in an annular region centered on the origin and open about the positive real axis

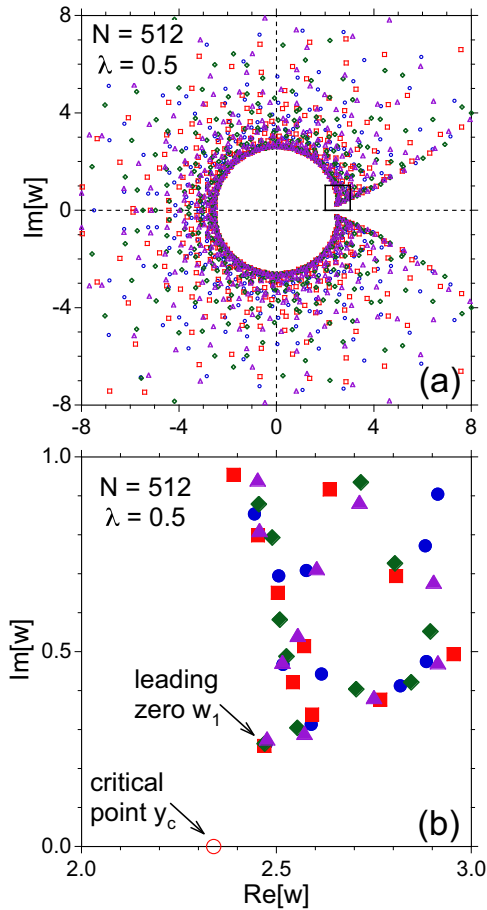


FIG. 1. Partition function zeros in the complex w plane for an $N = 512$ HS chain tethered to an attractive wall with $\lambda = 0.5$. Four data sets, obtained from four separate simulations, are shown with different symbols and colors. Although the individual zeros are not reproduced between simulations, the boundaries defining the distribution of the zeros and the leading zeros are well reproduced. Panel (b) shows an enlargement of the boxed region in (a) detailing the neighborhood of the leading zero w_1 and illustrating its reproducibility. The location of the critical point y_c , as determined by our finite-size-scaling analysis, is also indicated.

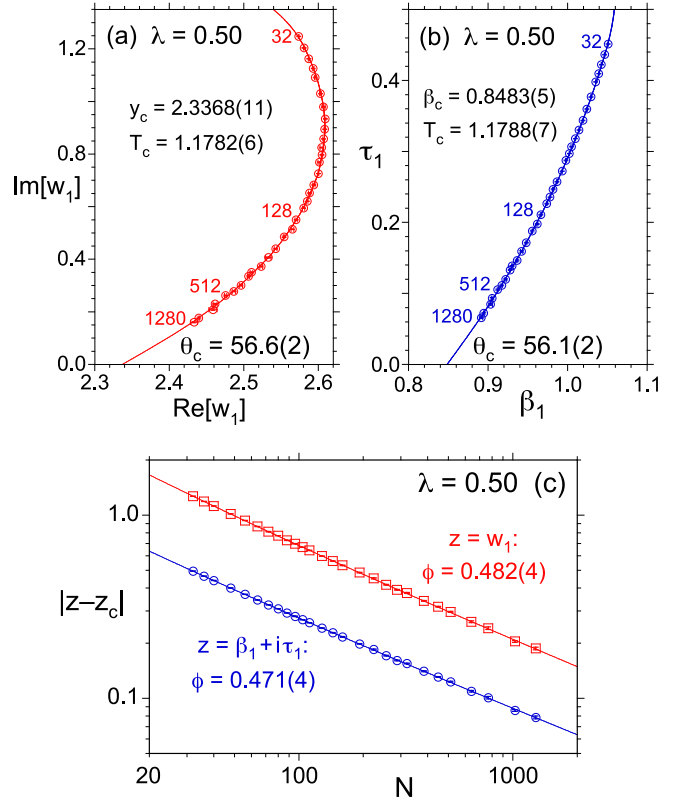


FIG. 2. Finite-size scaling analysis of the leading partition function zeros for a HS chain tethered to an attractive wall with $\lambda = 0.5$. [(a) and (b)] The leading zeros for $32 \leq N \leq 1280$ in the $z = w_1$ and $z = \beta_1 + i\tau_1$ complex planes, respectively. Values for the critical point y_c and β_c and the approach angle θ_c , obtained by fitting to Eq. (10), are shown. (c) Absolute distance from the critical point vs chain length N for the leading zeros shown above. Values of the crossover exponent ϕ , obtained by fitting to Eq. (12), are shown.

with the leading zero pinching down toward the real axis. On this plot we show, using different colors and symbols, the zeros obtained from four independent simulations. As seen here and previously noted [15,40], the exact locations in the complex plane of the individual zeros are not reproducible between simulations, however, both the boundaries separating regions with and without zeros and the leading zero are well reproduced. In Fig. 1(b) we show an enlargement of the partition function zero map that highlights the reproducibility of the leading zero. In our full data set for $N = 512$, $\lambda = 0.5$ we have 17 independent estimates of w_1 leading to a final value of $w_1 = 2.4755(15) + i0.2621(22)$ where the numbers in parentheses are the standard error in the last digits shown. In Fig. 1(b) we also include our result for the $N \rightarrow \infty$ adsorption critical point y_c (in part to illustrate that there is no simple extrapolation of the zero-map boundaries to y_c). The partition function zero maps for all the cases studied here have the same general appearance as Fig. 1 and this same structure is also seen for simple lattice models of an absorbing chain [17] and for the bond fluctuation lattice model [15].

In Figs. 2(a) and 2(b) we show the leading partition function zeros for chain lengths in the range $32 \leq N \leq 1280$ for the case of $\lambda = 0.5$ in the $z = w$ and $z = \beta + i\tau$ complex planes, respectively. With increasing chain length N these

TABLE I. Adsorption transition properties as obtained from the leading partition function zeros for a HS chain tethered to an attractive surface with range $\lambda\sigma$ and for a BF lattice chain. Included are the transition temperature T_c , approach angle θ_c , and crossover exponent ϕ , all computed using a correction-to-scaling exponent $\Delta = 0.5$.

	w plane			$\beta\tau$ plane		
	T_c (ϵ/k_B)	θ_c ($^\circ$)	ϕ	T_c (ϵ/k_B)	θ_c ($^\circ$)	ϕ
$\lambda = 0.01$	0.2228(1)	55.8(3)	0.491(6)	0.2229(1)	54.4(3)	0.473(5)
$\lambda = 0.10$	0.4467(2)	56.3(2)	0.489(4)	0.4471(2)	55.1(2)	0.472(3)
$\lambda = 0.50$	1.1782(6)	56.6(2)	0.482(4)	1.1788(7)	56.1(2)	0.471(4)
$\lambda = 1.00$	2.410(2)	57.7(2)	0.491(3)	2.408(2)	57.8(2)	0.481(3)
$\lambda = 2.00$	5.834(7)	58.6(2)	0.469(4)	5.825(8)	58.8(2)	0.464(4)
BF-lattice	1.0291(6)	57.6(2)	0.489(3)	1.0291(6)	57.3(2)	0.480(3)

leading zeros are seen to approach the positive real axis along a curving arc, consistent with the Yang-Lee picture of a phase transition. In the asymptotic limit this approach toward the real axis is expected to be linear, and thus the curvature seen here indicates that corrections to scaling are required in our analysis. The solid lines in Figs. 2(a) and 2(b) are weighted fits to the Eq. (10) scaling relation assuming $\Delta = 0.5$. From these three-parameter fits we obtain the critical point location y_c or β_c and the approach angle θ_c of the leading zeros to the critical point as shown in the plots and given in Table I. The two different complex planes give results for T_c and θ_c in good agreement despite the fact that the corrections to scaling are seen to be much stronger in the complex w plane. Results for the other interaction ranges λ (using $32 \leq N \leq 1024$ for $\lambda = 0.01, 0.1, 1.0$ and $64 \leq N \leq 1024$ for $\lambda = 2.0$) as well as for the bond-fluctuation lattice model (using $32 \leq N \leq 1536$) are also given in Table I. We use weighted fits in the determination of T_c and θ_c , except for the cases of $\lambda = 1.0$ and 2.0 where we require unweighted fits for agreement between the w plane and $\beta\tau$ -plane constructions. For the HS chains a larger interaction range λ gives a higher transition temperature T_c while the approach angle θ_c is approximately constant across all λ (although this angle does show a systematic increase with increasing λ). The BF lattice results are quite similar to the $\lambda = 0.5$ continuum results, consistent with the structure of this lattice model [15].

Having located the critical point, we now use the Eq. (12) scaling relation to obtain the crossover exponent ϕ as shown in Fig. 2(c). Although not as evident as in Figs. 2(a) and 2(b), corrections to scaling are essential to accurately fit these data. Results for ϕ from these three-parameter fits, shown in the plot and given in Table I, are close but do not overlap within uncertainty. Similar results are obtained for the other λ values as shown in Table I. We systematically find the ϕ estimates from the w -plane analysis to be slightly larger than the estimates from the inverse temperature plane. Averaging the results over the different λ values (including the BF lattice result) gives $\phi = 0.485(8)$ for the w plane and $\phi = 0.474(6)$ for the inverse temperature plane. The uncertainties given are the standard deviations between the values in each data set which are seen to be comparable to the individual error estimates. These average results for the two complex planes do agree within uncertainty and an average over the full set of values gives $\phi = 0.479(9)$.

For the fits shown in Fig. 2 and for the corresponding analysis used to compute the data given in Table I we have

assumed a correction-to-scaling exponent of $\Delta = 0.5$. To investigate the validity of this assumption, we have also treated Δ as an adjustable parameter. The results, presented and discussed in the Appendix, lead us to conclude that $\Delta = 0.5$ is a reasonable value that will be adopted throughout this work.

In Fig. 3(a) we provide another view of the leading partition function zeros in the complex inverse temperature plane, plotting $\tau_1(N)$ vs $\beta_1(N) - \beta_c$ for the full set of interaction ranges λ and for the BF lattice model (using our $\beta_c = 1/T_c$ values from Table I). The lines are fits to the Eq. (10) scaling relation (adapted to the $\beta\tau$ -complex plane). This plot

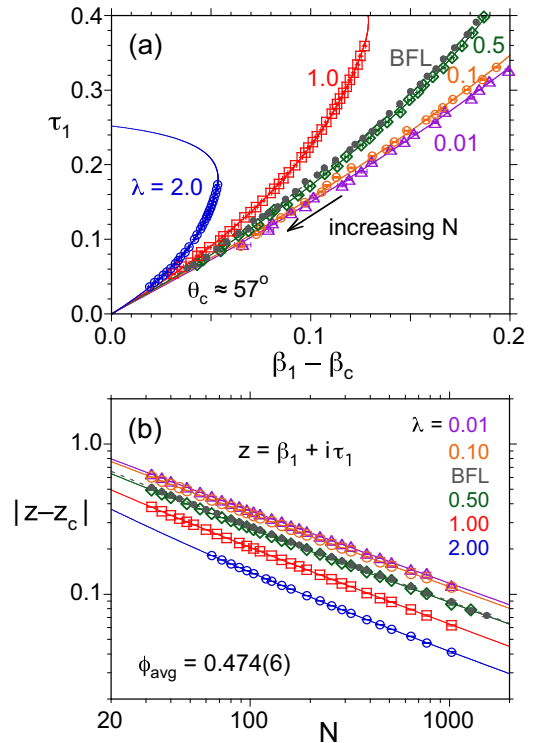


FIG. 3. (a) Approach of the leading partition function zeros toward the critical point β_c in the $z = \beta_1 + i\tau_1$ complex plane. Results are shown for the tethered HS chain (open symbols) with different surface SW interaction ranges λ , as indicated, and also for the BF-lattice model (filled symbols). Values for $\beta_c = \epsilon/k_B T_c$ are from Table I and the lines are fits to Eq. (10), adapted for the $\beta\tau$ plane. (b) Absolute distance from the critical point vs chain length N for the leading zeros shown above. Values of the crossover exponent ϕ , obtained by fitting to Eq. (12), are given in Table I.

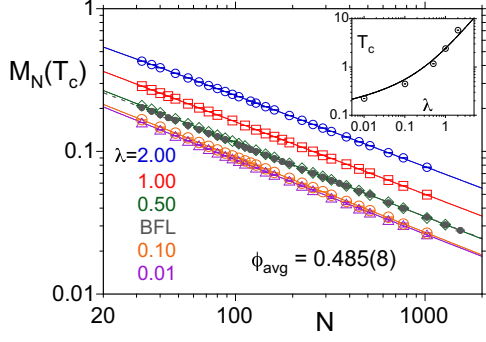


FIG. 4. Chain-adsorption order parameter $M_N(T_c)$ vs length N for a tethered HS chain (open symbols) with different surface SW interaction ranges λ and for the BF-lattice model (filled symbols) using T_c values given in Table I. Shown from top to bottom are $\lambda = 2.0, 1.0, 0.5, \text{BFL}, 0.1,$ and 0.01 . The lines are fits to the Eq. (16) scaling relation (which includes corrections to scaling) and the resulting ϕ values are given in Table II. Inset: Transition temperature T_c vs SW interaction range λ . Symbols are from Table I while the solid line is the simple analytic expression for the Boyle temperature for the monomer-surface interaction.

illustrates the universality of the approach angle θ_c and also shows that corrections scaling, as assessed by the curvature in each data set, become larger with increasing λ . The systematic increase we observe in θ_c with λ may result from these stronger corrections to scaling, suggesting the need for larger N values for larger λ to capture the correct asymptotic behavior. In Fig. 3(b) we present scaling plots of the absolute distance from the critical point $|z - z_c|$ vs N for the data in Fig. 3(a). The lines are fits to Eq. (12) and the resulting ϕ values are given in Table I.

As a consistency check on our approach we have also determined the crossover exponent ϕ from the scaling behavior of the order parameter $M_N(T)$ [Eq. (6)] at $T = T_c$ given (including lowest-order correction to scaling) by

$$M_N(T_c) = a_M N^{\phi-1} (1 + c_M N^{-\Delta}), \quad (16)$$

where a_M and c_M are constants. This is a standard approach for computing ϕ but it is known to be very sensitive to the correct value of T_c . Using the critical temperatures obtained from our partition function zero analysis (given in Table I) we have constructed $M_N(T_c)$ vs N scaling plots shown in Fig. 4 for the HS chain with different λ and for the BF lattice model. The resulting crossover exponents are given in Table II (where the uncertainty is primarily due to the uncertainty in T_c) and seen to be in reasonable agreement with values given in Table I. The largest discrepancy is for the $\lambda = 2.0$ case where we have the largest corrections to scaling.

Finally, we examine the determination of the crossover exponent ϕ using only the imaginary part of the leading partition function zeros. Since the imaginary part of the Eq. (9) scaling relation does not include y_c (or β_c), ϕ can, in principle, be obtained via the scaling of $\text{Im}[w_1(N)]$ [or $\tau_1(N)$] with N without knowledge of the transition temperature. In practice, we find that this approach gives reasonable results for the $\tau_1(N)$ zeros but appears to be inaccurate when working with the zeros from the complex w plane. In Fig. 5(a) we show scaling plots of

TABLE II. Crossover exponent ϕ obtained from the scaling of the order parameter $M_N(T_c)$ and leading zero $\tau_1(N)$ with chain size N [Figs. 4 and 5(a), respectively], and from extrapolation of the $\tau_1(N)$ -ratio estimates for $\phi_{\text{eff}}(N)$ [Fig. 5(b)]. The τ_1 methods do not require knowledge of the transition temperature T_c .

	$M_N(T_c)$ scaling	$\tau_1(N)$ scaling	$\tau_1(N)$ ratio
$\lambda = 0.01$	0.485(3)	0.474(5)	0.483(3)
$\lambda = 0.10$	0.473(3)	0.475(4)	0.480(3)
$\lambda = 0.50$	0.480(3)	0.468(5)	0.478(2)
$\lambda = 1.00$	0.492(4)	0.479(4)	0.479(1)
$\lambda = 2.00$	0.494(4)	0.459(5)	0.480(1)
BF-lattice	0.488(3)	0.481(4)	0.483(2)

$\tau_1(N)$ vs N for the HS chain and BFL models. The resulting ϕ values, given in Table II, are seen to be in good agreement with the values from our full leading-zero analysis given in Table I. We note that the correction-to-scaling contribution included in Eq. (9) is needed for accurate fitting of these data. The analogous scaling plot for $\text{Im}[w_1(N)]$ vs N (not shown) gives some results quite inconsistent with those we have obtained by our other methods and thus does not appear reliable.

A related approach for obtaining ϕ is based on the finite-size approximates $\phi_{\text{eff}}(N)$ built from ratios of $\text{Im}[w_1(N)]$ or $\tau_1(N)$ [see Eq. (14)]. In Fig. 5(b) we plot $\phi_{\text{eff}}(N)$ [built from

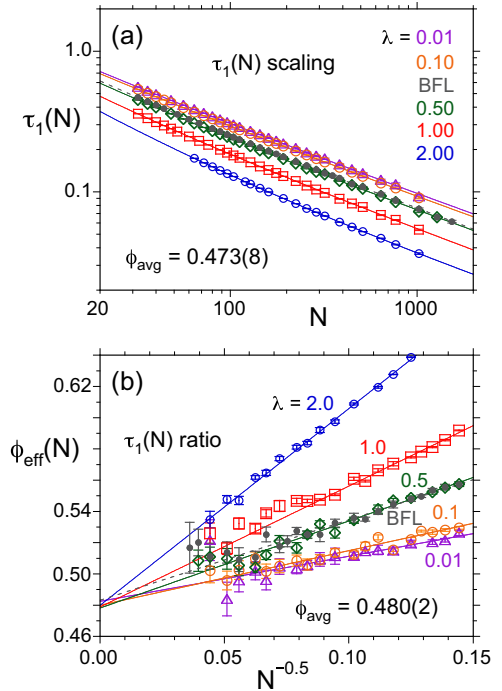


FIG. 5. Determination of the crossover exponent ϕ from the leading zeros $\tau_1(N)$. Results are shown for the tethered HS chain (open symbols) with surface SW interaction range λ , as indicated, and for the BF-lattice model (filled symbols). (a) $\tau_1(N)$ vs chain length N , where the lines are fits to the imaginary part of the Eq. (9) scaling relation, adapted for the $\beta\tau$ plane. (b) Effective crossover exponent $\phi_{\text{eff}}(N)$ [given by Eq. (14) with $z = \beta_1 + i\tau_1$] vs $N^{-1/2}$, where the lines are weighted linear fits in $N^{-1/2}$ as given by Eq. (15). Average ϕ values are shown while the individual ϕ values are given in Table II.

$\tau_1(N)]$ vs $N^{-1/2}$ for the HS chain and BFL models. These data display linear behavior as expected from Eq. (15) and extrapolate to similar asymptotic ϕ values (given in Table II) in the limit of $N \rightarrow \infty$. The slopes of the linear fits are proportional to the correction-to-scaling amplitude and thus, as expected from Fig. 3(a), we find that the corrections to scaling increase with increasing λ . The analogous plot for $\phi_{\text{eff}}(N)$ built from $\text{Im}[w_1(N)]$ vs $N^{-1/2}$ (not shown) gives results with pronounced curvature and thus the linear fit of Eq. (15) is not applicable. Using a quadratic fit for the $N \rightarrow \infty$ extrapolation gives some results quite inconsistent with those we have obtained by other methods, so again, we do not consider this $\phi_{\text{eff}}(N)$ approach using the $\text{Im}[w_1(N)]$ zeros to be reliable.

IV. DISCUSSION AND CONCLUSIONS

In this work we have studied the thermodynamics of the adsorption of a flexible polymer chain onto an attractive flat surface by analyzing the trajectory of the leading partition function zeros ($z_1 = w_1$ or $\beta_1 + i\tau_1$) through the complex plane toward the transition critical point z_c . By fitting this trajectory to a scaling relation that includes a lowest-order correction-to-scaling contribution we are able to locate the critical point and determine the angle of approach θ_c of the leading zeros toward this point. The latter angle is a universal quantity for this transition. Once we have identified the critical point we analyze the variation of the absolute distance $|z_1(N) - z_c|$ with chain length N to obtain the crossover exponent ϕ , another universal descriptor of this transition. We have carried out this analysis for a tangent-HS chain adsorbing onto a hard surface with a SW potential of width $\lambda\sigma$ with $0.01 \leq \lambda \leq 2.0$. The transition temperature increases by a factor of 26 across this range of interaction lengths while the approach angle and crossover exponent give values of $\theta_c = 56.7(1.5)^\circ$ and $\phi = 0.478(10)$. The limitation of our analysis for the continuum chain to $N \leq 1280$ is set by our computational resources. The computational demands of the WL simulations depend on both N and the histogram flatness level (where the latter controls the precision of the calculation). As previously noted, we use a rich move set in these simulations to facilitate the exploration of the full configurational phase space. However, since for the longer chains we do not take the simulation all the way to the ground state, a simplified move set with just the axial rotate and pivot moves should suffice in these cases. This would improve the simulation efficiency and thus potentially allow for the study of longer chains.

We have also applied the above analysis to the bond-fluctuation lattice model which we have previously studied [15]. In that earlier work we did not systematically implement corrections to scaling in our determination T_c and ϕ . We assumed a quadratic leading-root trajectory in the complex plane which underestimates the transition temperature and we restricted our analysis to the imaginary part of the leading zeros to find ϕ . It is clear now that a systematic application of corrections to scaling is essential to accurately model the data for the N range assessable through our simulation methods. Our new results for the BF lattice model are $\theta_c = 57.5(2)^\circ$, $T_c = 1.0291(6)$, and $\phi = 0.485(5)$ which are in agreement with Hsu's results, obtained via PERM for chains up to $N = 10\,000$, of $T_c = 1.0298(3)$, and $\phi = 0.487(5)$ [52].

Our best estimate of the crossover exponent, obtained by averaging over our HS chain results for different λ and our BFL chain results, is $\phi = 0.479(9)$. As a check we have also computed ϕ from the scaling of $M_N(T_c)$, using the T_c values from the partition function zero analysis, and obtain $\phi = 0.485(8)$. These results are in agreement with the several recent estimates obtained by different methods for an absorbing self-avoiding walk on a simple cubic lattice model which include $\phi = 0.484(2)$ (Grassberger [8]), $0.483(3)$ (Klushin *et al.* [13]), $0.492(4)$ (Plascak *et al.* [18]), and $0.485(6)$ (Bradly *et al.* [19]). Thus our result for ϕ is both internally self-consistent and, more importantly, is consistent with the universality of this exponent across both lattice and continuum models.

A second exponent called δ was introduced in Luo's analysis of the polymer adsorption transition [11]. This exponent plays the role of the correlation length exponent ν in magnetic systems and, in finite-size scaling theory [48,50], it describes the shift of a transition away from the true critical temperature T_c due to finite system size via the scaling relation (with lowest-order corrections to scaling)

$$T_c^{(N)} - T_c = a_T N^{-1/\delta} (1 + c_T N^{-\Delta}). \quad (17)$$

In terms of inverse temperature Eq. (17) reads (to first order in $N^{-1/\delta}$)

$$\left| \frac{1}{T_c^{(N)}} - \frac{1}{T_c} \right| = \frac{a_T}{T_c^2} N^{-1/\delta} (1 + c_T N^{-\Delta}). \quad (18)$$

If we continue Eq. (18) into the complex plane, taking the leading zeros as finite-size estimates of the transition point such that $1/T_c^{(N)} = \beta(N) + i\tau(N)$, we obtain on comparison with the $\beta\tau$ version of Eq. (12) the exponent identity $1/\delta = \phi$. [Alternatively, the same result is obtained by simply identifying Eq. (18) with the real part of the $\beta\tau$ version of Eq. (9)]. This connection between the exponents δ and ϕ for the adsorption of a self-avoiding walk has been demonstrated previously by both Bradley *et al.* [19] and by Martins *et al.* [20] using different methods.

Our best estimate for the approach angle of the leading partition function zeros toward the critical point, obtained by averaging over our HS chain results for different λ and our BFL chain results, is $\theta_c = 56.8(1.4)^\circ$. This value falls within Janse van Rensburg's estimated bounds on θ_c of $54.6^\circ \rightarrow 64.0^\circ$ for an absorbing self-avoiding walk on a simple cubic lattice [17]. These bounds were obtained by fitting $\text{Re}[w_1(N)]$ vs $\text{Im}[w_1(N)]$ to a simple parabola [i.e., Eq. (11) with $\phi = \Delta$] with the smaller angle resulting from forcing the fit to match the known critical point. We have a much tighter bound on this approach angle due to our inclusion of correction-to-scaling contributions in our analysis. Again, our results are consistent with the universality of this angle across both lattice and continuum models. Also, we have obtained this approach angle in both the complex w and $\beta\tau$ planes and find agreement between the two constructions, consistent with the conformal mapping relating w and $\beta + i\tau$. Gordillo-Guerrero *et al.* have carried out a related study of the Fisher zero approach angle to the critical point for the three-dimensional (3D) Ising model [51]. In that work finite-size estimates for the approach angle were obtained from the first two leading zeros (working in the $u = w^{-4}$ complex plane) giving an extrapolated value of

$\theta_c^{3D\text{-Ising}} = 59.2(1.0)^\circ$. Thus, the polymer adsorption approach angle is quite similar to the 3D Ising model result, although the two systems are not in the same universality class.

The continuum model studied in this work allows us to investigate the effects of interaction range on the polymer adsorption transition. In particular, we are able to study a continuous range of λ values, including $\lambda < \sigma$, which is not possible in a lattice model. With decreasing interaction range λ the adsorption transition moves to lower temperature similar to what is observed for the polymer collapse transition for a flexible SW chain [53]. However, unlike the polymer collapse case, where the transition changes from continuous to discontinuous for sufficiently small interaction range, there is no such change in the character of the adsorption transition. Comparing the results for $\lambda = 0.1$ and 0.01 in Figs. 3–5 there appears to be a limiting behavior for the leading partition function zeros and $M_N(T_c)$ as $\lambda \rightarrow 0$ (and $T_c \rightarrow 0$).

Klushin *et al.* [13] have studied the effects of interaction range on the adsorption transition for a self-avoiding walk on a simple cubic lattice. For such a lattice model the possible interaction ranges are given by integer multiples of the lattice spacing with the minimum range being one lattice unit (whereas in the continuum model we are able to study interaction ranges smaller than the monomer diameter σ). For a variation in interaction range W from 1 to 10 lattice units, Klushin *et al.* find a 24-fold increase in T_c that is well described by a power-law relation $T_c \sim (W + 1/2)^{1/\nu}$ where $\nu = 3/5$ is the Flory exponent. In the inset to Fig. 4 we show the variation of T_c with interaction range λ for our continuum model. A power-law relation would give linear behavior in this log-log plot, which is clearly not the case (at least for $\lambda < 1$). To describe the variation of T_c with λ in the continuum model we will make an analogy with the polymer collapse transition, where in the long chain limit the collapse temperature is approximately given by the monomer-monomer Boyle temperature [53]. Thus we consider a second-virial-like coefficient for the monomer-surface interaction

$$B_2(T) = \int_{-\sigma/2}^{\infty} [1 - e^{-u(z)\beta/\epsilon}] dz = \frac{\sigma}{2} + \lambda\sigma(1 - e^\beta), \quad (19)$$

where $u(z) = \infty$ for $z < 0$. B_2 vanishes at the Boyle temperature $T_B = \epsilon/k_B \ln[1 + 1/2\lambda]$. We include $T_B(\lambda)$ in the Fig. 4 inset where it is seen to provide a rough estimate of T_c for the continuum chain model. For larger λ this T_B does not map onto the lattice power-law form for T_c given above. However, for larger λ , a blob with size proportional to λ will take on the role of a monomer [13,54]. For a blob containing N_b monomers, with blob size $R_b \sim N_b^\nu$, we obtain $B_2(T) \approx \lambda\sigma/2 + \lambda\sigma(1 - e^{N_b\beta})$ leading to the prediction $T_B \sim \lambda^{1/\nu}$ in agreement with the lattice model finding. The larger corrections to scaling we observe for $\lambda = 2.0$, and which are also observed for the lattice model with increasing W [13], may be a reflection of this changeover from a monomer to a blob controlled process. If the basic adsorption unit is a blob, for which the adsorbed layer will no longer be a simple monolayer, then one might anticipate that longer chains are required to capture the same asymptotic behavior (even when corrections to scaling are included) than for the case of the single monomer adsorption unit.

Finally, we comment on the range of the values for the crossover exponent ϕ obtained in this work (collected in Tables I and II). In particular, for each λ in Table I the two ϕ estimates, which come from the same leading partition function zeros represented in two different ways, do not agree within the estimated statistical uncertainties. For sufficiently long chains these results must be identical, however, here we clearly see finite-size effects despite the fact that we have included corrections to scaling in our analysis. The mapping between the w and $\beta\tau$ planes for Eqs. (10) and (12) should preserve the fit parameters m, c, A, B with $A \rightarrow A/y_c$. Our results show the m and A parameters to be reasonably well preserved, however, the c and B parameters, which set the amplitude of the correction-to-scaling term, are not preserved in the mapping. The correction-to-scaling term is really an effective correction that includes all higher-order contributions [48,49] and we find these contributions to be different in the w and $\beta\tau$ representations. In all cases we find the corrections to scaling to be smaller in the $\beta\tau$ plane. The variation between the w and $\beta\tau$ -plane estimates for ϕ are larger than the estimated statistical uncertainty in the individual estimates, despite the fact that our results for T_c agree within uncertainty for the two approaches. Similarly, our ϕ results obtained for $M_N(T_c)$, which rely on the T_c values for the partition function zero analysis, are close to the w -plane values while, as might be expected, the values obtained solely from the $\tau_1(N)$ roots are similar to our $\beta\tau$ -plane results. Thus, the scatter in all of our ϕ results is larger than the statistical uncertainty estimated for each individual value. This type of behavior has been studied in detail by Bradly *et al.* [19] for the adsorption of a lattice polymer in both 2D and 3D systems. These authors show that different methods for obtaining T_c lead to different estimates for ϕ for which the statistical uncertainty can be smaller than the variation between the ϕ values. (These results are quite striking for the 2D square lattice where the exact value of ϕ is known.) Thus, Bradly *et al.* suggest carrying out this type of calculation using a number of approaches and then averaging over results from all methods to both obtain a final result and a realistic uncertainty estimate. For the results presented in Table I we have no strong reason to prefer one complex plane construction over the other (noting that they yield essentially the same critical temperatures) and thus we feel that averaging over the results from the two constructions is reasonable.

Of course, as shown in our Fig. 5 results, the partition function zero method does allow the computation of ϕ without knowledge of T_c . However, for our range of N values, we find that while the $\tau_1(N)$ roots give consistent results for ϕ the $\text{Im}[w_1(N)]$ roots are not reliable for this calculation. There are two issues that likely contribute here. First, each τ is built from both the real and imaginary parts of w so it encodes more w -plane information than just $\text{Im}[w_1(N)]$ alone. Second, the $\beta\tau$ roots are subject to smaller corrections to scaling than the w roots. Finally, we note that for our large N data the Eq. (14) ratio method produces very noisy $\phi_{\text{eff}}(N)$ values due to an amplification of uncertainty [see Fig. 5(b)], making it a somewhat less attractive approach. On the other hand, the ratio method does highlight the importance of corrections to scaling, which are not obvious in the direct scaling plot of Fig. 5(a). The construction used in Fig. 5(b) also allows us to put bounds on the correction-to-scaling exponent Δ , since

TABLE III. Optimal correction-to-scaling exponent Δ_{opt} obtained by treating Δ as an additional fit parameter in the Eq. (10) analysis of the leading partition function zeros for a HS chain tethered to an attractive surface with range $\lambda\sigma$ and for a BF lattice chain.

	Δ_{opt}	
	w plane	$\beta\tau$ plane
$\lambda = 0.01$	0.50(5)	0.51(12)
$\lambda = 0.10$	0.49(4)	0.46(9)
$\lambda = 0.50$	0.50(3)	0.50(5)
$\lambda = 1.00$	0.46(3)	0.36(5)
$\lambda = 2.00$	0.36(4)	0.27(5)
BF-lattice	0.53(3)	0.53(6)

the lines for different λ are expected to intersect at $N^{-\Delta} = 0$. Varying Δ moves the intersection location of these lines and we find that the intersection region overlaps $N^{-\Delta} = 0$ for the range $0.48 < \Delta < 0.55$.

ACKNOWLEDGMENTS

Financial support from Hiram College and the National Science Foundation (Grant No. DMR-1607143) is gratefully acknowledged.

APPENDIX: CORRECTION-TO-SCALING EXPONENT

Throughout the data analysis presented in Sec. III, we have assumed a correction-to-scaling exponent of $\Delta = 0.5$. To investigate the validity of this assumption we have carried out curve fits to Eq. (10) (and its $\beta\tau$ -plane analog) in which Δ is treated as free parameter. The resulting best fit Δ values are listed in Table III as Δ_{opt} . In the majority of cases $\Delta = 0.5$ falls within the uncertainty range of these best fit Δ_{opt} values. These results for Δ_{opt} are based on the minimization of the chi-squared function $\chi^2(y_c, m, c, \Delta)$ and in all cases we find the minima in χ^2 to be relatively insensitive to variation in Δ in the neighborhood of $\Delta = 0.5$ (as has been noted in lattice studies of polymer adsorption [8,18,20,21]), with the difference between the optimal fit parameters and those obtained using $\Delta = 0.5$ being rather modest. Also, in such multiparameter fits there can be strong correlation between the adjustable parameters. For example, for the cases of $\lambda = 1.0$ and 2.0 , holding the approach angle fixed to $\theta_c = 58.0^\circ$ ($m = 0.625$) moves the fit results for Δ_{opt} into the range 0.47 – 0.51 . Thus, we consider the choice of $\Delta = 0.5$ to be reasonable and, both for clarity of presentation and consistency with previous work, we have chosen to use this value for all of our reported results. Note that we want to fix Δ to allow for higher precision estimates of the other fit parameters.

-
- [1] R. R. Netz and D. Andelman, *Phys. Rep.* **380**, 1 (2003).
 - [2] E. Eisenriegler, K. Kremer, and K. Binder, *J. Chem. Phys.* **77**, 6296 (1982).
 - [3] H. Meirovitch and S. Livne, *J. Chem. Phys.* **88**, 4507 (1988).
 - [4] R. Hegger and P. Grassberger, *J. Phys. A: Math. Gen.* **27**, 4069 (1994).
 - [5] S. Metzger, M. Müller, K. Binder, and J. Baschnagel, *Macromol. Theory Simul.* **11**, 985 (2002).
 - [6] E. J. Janse van Rensburg and A. R. Rechnitzer, *J. Phys. A: Math. Gen.* **37**, 6875 (2004).
 - [7] R. Decas, J.-U. Sommer, and A. Blumen, *J. Chem. Phys.* **120**, 8831 (2004).
 - [8] P. Grassberger, *J. Phys. A: Math. Gen.* **38**, 323 (2005).
 - [9] R. Decas, J.-U. Sommer, and A. Blumen, *Macromol. Theory Simul.* **17**, 429 (2008).
 - [10] J. Luettmer-Strathmann, F. Rampf, W. Paul, and K. Binder, *J. Chem. Phys.* **128**, 064903 (2008).
 - [11] M.-B. Luo, *J. Chem. Phys.* **128**, 044912 (2008).
 - [12] H.-P. Hsu and K. Binder, *Macromolecules* **46**, 2496 (2013).
 - [13] L. I. Klushin, A. A. Polotsky, H.-P. Hsu, D. A. Markelov, K. Binder, and A. M. Skvortsov, *Phys. Rev. E* **87**, 022604 (2013).
 - [14] J. Luettmer-Strathmann and K. Binder, *J. Chem. Phys.* **141**, 114911 (2014).
 - [15] M. P. Taylor and J. Luettmer-Strathmann, *J. Chem. Phys.* **141**, 204906 (2014).
 - [16] E. J. Janse van Rensburg, *J. Stat. Mech.* (2016) P033202.
 - [17] E. J. Janse van Rensburg, *J. Stat. Mech.* (2017) P033208.
 - [18] J. A. Plascak, P. H. L. Martins, and M. Bachmann, *Phys. Rev. E* **95**, 050501(R) (2017).
 - [19] C. J. Bradly, A. L. Owczarek, and T. Prellberg, *Phys. Rev. E* **97**, 022503 (2018).
 - [20] P. H. L. Martins, J. A. Plascak, and M. Bachmann, *J. Chem. Phys.* **148**, 204901 (2018).
 - [21] C. J. Bradly, A. L. Owczarek, and T. Prellberg, *Phys. Rev. E* **98**, 062141 (2018).
 - [22] S. Bhattacharya, V. G. Rostiashvili, A. Milchev, and T. A. Vilgis, *Phys. Rev. E* **79**, 030802(R) (2009).
 - [23] S. Bhattacharya, V. G. Rostiashvili, A. Milchev, and T. A. Vilgis, *Macromolecules* **42**, 2236 (2009).
 - [24] A. Milchev and K. Binder, *Phys. Rev. Lett.* **123**, 128003 (2019).
 - [25] A. Milchev and K. Binder, *J. Chem. Phys.* **152**, 064901 (2020).
 - [26] A. N. Semenov, *Eur. Phys. J. E* **9**, 353 (2002).
 - [27] M. Deng, Y. Jiang, H. Liang, and J. Z. Y. Chen, *J. Chem. Phys.* **133**, 034902 (2010).
 - [28] D. Welch, M. P. Letting, M. Ripoll, Z. Dogic, and G. A. Vlieghenart, *Soft Matter* **11**, 7507 (2015).
 - [29] C. N. Yang and T. D. Lee, *Phys. Rev.* **87**, 404 (1952).
 - [30] T. D. Lee and C. N. Yang, *Phys. Rev.* **87**, 410 (1952).
 - [31] M. E. Fisher, in *Statistical Physics, Weak Interactions, Field Theory*, edited by W. E. Brittin, Lectures in Theoretical Physics, Vol. 7C (University of Colorado Press, Boulder, 1965) Chap. 1.
 - [32] C. Itzykson, R. B. Pearson, and J. B. Zuber, *Nucl. Phys. B* **220**, 415 (1983).
 - [33] I. Bena, M. Droz, and A. Lipowski, *Int. J. Mod. Phys. B* **19**, 4269 (2005).
 - [34] R. Finsy, M. Janssens, and A. Bellemans, *J. Phys. A: Math. Gen.* **8**, L106 (1975).
 - [35] D. C. Rapaport, *J. Phys. A: Math. Gen.* **10**, 637 (1977).
 - [36] V. Privman and D. A. Kurtze, *Macromolecules* **19**, 2377 (1986).
 - [37] N. A. Alves and U. H. E. Hansmann, *Phys. Rev. Lett.* **84**, 1836 (2000).
 - [38] J. H. Lee, S.-Y. Kim, and J. Lee, *J. Chem. Phys.* **133**, 114106 (2010).

- [39] J. H. Lee, S.-Y. Kim, and J. Lee, *Phys. Rev E* **86**, 011802 (2012).
- [40] M. P. Taylor, P. P. Aung, and W. Paul, *Phys. Rev. E* **88**, 012604 (2013).
- [41] D. Foster, R. Kenna, and C. Pinettes, *Entropy* **21**, 153 (2019).
- [42] F. Wang and D. P. Landau, *Phys. Rev. Lett.* **86**, 2050 (2001).
- [43] F. Wang and D. P. Landau, *Phys. Rev. E* **64**, 056101 (2001).
- [44] M. P. Taylor, W. Paul, and K. Binder, *Polymer Sci., Ser. C* **55**, 23 (2013).
- [45] M. S. Causo, *J. Stat. Phys.* **108**, 247 (2002).
- [46] F. A. Escobedo and J. J. de Pablo, *J. Chem. Phys.* **102**, 2636 (1995).
- [47] M. P. Taylor, *Macromolecules* **50**, 6967 (2017).
- [48] D. P. Landau, *Physica A* **205**, 41 (1994).
- [49] B. Li, N. Madras, and A. D. Sokal, *J. Stat. Phys.* **80**, 661 (1995).
- [50] D. P. Landau and K. Binder, *Monte Carlo Simulations in Statistical Physics* (Cambridge University, Cambridge, UK, 2000).
- [51] A. Gordillo-Guerrero, R. Kenna, and J. J. Ruiz-Lorenzo, *J. Stat. Mech.* (2011) P09019.
- [52] H.-P. Hsu, Private communication (2013).
- [53] M. P. Taylor, W. Paul, and K. Binder, *J. Chem. Phys.* **131**, 114907 (2009).
- [54] P.-G. de Gennes, *Scaling Concepts in Polymer Physics* (Cornell University Press, Ithaca, NY, 1979).